

# A non-conserving coagulation model with extremal dynamics

**Róbert Juhász**

Research Institute for Solid State Physics and Optics, H-1525 Budapest, P.O.Box 49, Hungary

E-mail: juhasz@szfki.hu

**Abstract.** A coagulation process is studied in a set of random masses, in which two randomly chosen masses and the smallest mass of the set multiplied by some fixed parameter  $\omega \in [-1, 1]$  are iteratively added. Besides masses (or primary variables), secondary variables are also considered that are correlated with primary variables and coagulate according to the above rule with  $\omega = 0$ . This process interpolates between known statistical physical models: The case  $\omega = -1$  corresponds to the strong disorder renormalisation group transformation of certain disordered quantum spin chains whereas  $\omega = 1$  describes coarsening in the one-dimensional Glauber-Ising model. The case  $\omega = 0$  is related to the renormalisation group transformation of a recently introduced graph with a fat-tail edge-length distribution. In the intermediate range  $-1 < \omega < 1$ , the exponents  $\alpha_\omega$  and  $\beta_\omega$  that characterise the growth of the primary and secondary variable, respectively, are accurately estimated by analysing the differential equations describing the process in the continuum formulation. According to the results, the exponent  $\alpha_\omega$  varies monotonically with  $\omega$  while  $\beta_\omega$  has a maximum at  $\omega = 0$ .

PACS numbers: 05.40.-a, 68.43.Jk, 05.10.Cc

## 1. Introduction

Coagulation processes arise in various areas of physics; one may think of polymerisation, growth of ordered domains in non-equilibrium magnetic systems [1], dynamics of droplets when water condenses on non-wetting surfaces [2], etc. The substance, or “mass” that aggregates is very frequently not conserved during the process: for example, agglomerating insoluble inclusions in molten metal may be lost from the melt by attachment to the wall of the vessel [3]. Therefore the theoretical investigation of the kinetics of such non-conserving coagulation processes is of great importance. Moreover, the models developed for the description of such systems may show interesting behaviour: the Smoluchowsky equation with certain coagulation kernels exhibits gelation transition and, in general, even the simplest models with conserved mass may have non-trivial solutions, see e.g. Ref. [3] and references therein. Beside quite realistic ones, there is a special class of (possibly non-conserving) coagulation models where only the actually smallest one among the masses is active while the other masses are temporarily inert. This type of *extremal dynamics* can be regarded as a rough approximation for models where the reaction rates are decreasing functions of the mass of particles. In what follows, we shall survey three processes with extremal dynamics in detail. We mention, however, that models of this type have also been introduced in the context of dynamics of growing and coalescing droplets [2] or multispecies pair annihilation reactions [4].

In the one-dimensional Glauber-Ising model started from a random initial state at zero temperature, the domain walls move as independent random walkers and annihilate upon meeting. While the closest pairs of walls come together and annihilate, the other domain walls hardly move. A simplified model of evolution of distances  $X_i$  between adjacent walls can be formulated as follows [5, 6]. The shortest interval  $X_m$  is eliminated together with the two adjacent intervals  $X_1$  and  $X_2$  and replaced by  $\tilde{X} = X_1 + X_2 + X_m$ . As the density of walls tends to zero, the distributions of intervals at different times become self-similar, depending on a single time-dependent length scale, and the corresponding scaling function can be calculated exactly [5, 7, 8]. Another quantity of interest is the fraction of space which has never been traversed by a domain wall. The length  $Y_i$  of such parts of intervals transforms in the way  $\tilde{Y} = Y_1 + Y_2$  when the shortest interval is eliminated. The characteristic value of  $X$  depends on the fraction  $c$  of the initial intervals that have not yet been eliminated as  $X \sim c^{-\alpha}$ , obviously, with  $\alpha = 1$ , while it has been found that  $Y \sim c^{-\beta}$ , where the persistence exponent  $\beta = 0.82492412\dots$  is the zero of a transcendental equation [7]. In addition to this, the autocorrelation exponent has also been exactly calculated in this model [9]. To obtain this quantity, the overlap  $Z_i$  of an interval with its initial state that transforms as  $\tilde{Z} = Z_1 + Z_2 - Z_m$  had to be considered. Later, a generalisation of persistence has been studied in the same model, which required to introduce an auxiliary variable transforming as  $\tilde{Y} = Y_1 + Y_2 + pY_m$  [10]. Here, the generalised persistence exponent has been found to vary monotonically with the partial survival factor  $p$  in the range

$$-1 \leq p \leq 1.$$

The next example is the strong disorder renormalisation group transformation of inhomogeneous quantum spin chains [11]. Here, the degrees of freedom related to the largest coupling (a bond between neighbouring spins or a local external field) are eliminated one after the other. In terms of logarithmic couplings,  $X_i$ , the renormalisation rule generally reads as  $\tilde{X} = X_1 + X_2 - X_m$ , where  $\tilde{X}$  is a newly formed effective variable and  $X_1, X_2$  are variables adjacent to the smallest one,  $X_m$ . For the relation between these variables and the couplings in the particular Hamiltonians we refer the reader to Ref. [12]. A variable  $Y_i$  that transforms according to the rule  $\tilde{Y} = Y_1 + Y_2$  under such a renormalisation step can be interpreted in the case of a particular model, the transverse field Ising chain, as the magnetic moment of a spin. For this process with i.i.d. random initial variables  $X_i$ , which corresponds to critical spin chains, the distribution of  $X$  flows again to a fixed point where it shows scaling behaviour. The characteristic value of  $X$  increases in the course of the process as  $X \sim c^{-\alpha}$  with  $\alpha = 1/2$ , while the variable  $Y$  grows as  $Y \sim c^{-\beta}$  with  $\beta = (1 + \sqrt{5})/4 = 0.809016\dots$  [12]. Note that the coagulation rules in the above two models differ only in the sign of  $X_m$ , which leads to different exponents  $\alpha$  and  $\beta$ .

Our third example is a random graph where three edges emanate from each node, and which is built on a regular one-dimensional lattice by adding long edges in the following way. To each edge of the one-dimensional lattice that we call short edges, a random weight  $X_i$  is assigned. Defining the length of a path as the sum of weights of the edges it contains, the closest pair of nodes of degree 2 with respect to this metric is chosen and connected by an edge of unit weight. This step is then iterated until all nodes become of degree 3 [13]. For this graph, a renormalisation procedure can be formulated where loops are eliminated step by step in reversed order compared to the construction procedure. Formally, the short edge with the minimal weight  $X_m$  is eliminated together with the nodes it connects, as well as with the neighbouring short edges with weights  $X_1, X_2$  and a new effective short edge is formed with a weight calculated asymptotically as  $\tilde{X} = X_1 + X_2$ . According to numerical results, the characteristic value of effective weights grows as  $X \sim c^{-\alpha}$  with  $\alpha = 0.826(1)$  [13]. This exponent characterises at the same time the diameter of finite graphs with  $N$  nodes with respect to the above metric via  $D(N) \sim N^\alpha$ .

As can be seen, these seemingly different problems can be treated in a common framework and can be interpreted as coagulation processes with extremal dynamics. In the first example, the total sum of the variables  $X_i$  is conserved while in the latter two cases it is not. We will study in this work a coagulation model controlled by a parameter  $\omega$  that interpolates continuously between the first two models and incorporates the third one as a special case, as well. We are interested in the exponents  $\alpha_\omega$  and  $\beta_\omega$  for intermediate values of the parameter  $\omega$  and shall provide accurate estimates for  $\alpha_\omega$  that is obtained as the root of a transcendental equation while  $\beta_\omega$  is accurately determined by the numerical analysis of a system of non-linear differential equations. We shall see that  $\alpha_\omega$  varies monotonically between the corresponding values of the two marginal

models, while, unlike the generalised persistence exponent of the model with partial survival mentioned above [10], the exponent  $\beta_\omega$  shows a maximum when  $\omega$  is varied. As can be seen, the transformation rule of the variable  $Y$  does not depend directly on the parameter  $\omega$  but it is influenced indirectly via the correlations emerging between  $X$  and  $Y$ , the strength of which is controlled by  $\omega$ . Therefore our results may contribute to the understanding of the role of correlations in such models. Moreover, these investigations provide an accurate estimate for the diameter exponent of the graph quoted above, for which we obtain  $\alpha = 0.82617561$  in agreement with the previous numerical result.

The rest of the paper is organised as follows. In Section 2, the model and its continuum description is introduced. In Sections 3 and 4, the way of approximative determination of the exponents  $\alpha_\omega$  and  $\beta_\omega$  is presented. Some calculations are given in the Appendix. Finally, results are discussed in Section 5.

## 2. The model and its continuum formulation

### 2.1. Definition of the model

Let us consider a finite set of positive vectors  $V_i = (X_i, Y_i)$  indexed by the integers  $i = 1, 2, \dots, N$ . We assume, moreover, that  $N$  is odd. The vectors are independent, identically distributed random variables drawn from a continuous distribution  $\rho(X, Y)dXdY$ , for which we require that all moments exist. The first components  $X_i$  and the second components  $Y_i$  are called primary and secondary variables, respectively. Assume, furthermore, that  $\omega \in [-1, 1]$  is a fixed real number. Now, the following procedure is considered on this set. The vector  $V_m$  with the smallest primary variable is chosen and, at the same time, two further vectors  $V_i$  and  $V_j$  are chosen at random from the set. These three vectors are removed and a new vector  $\tilde{V}$  with components

$$\begin{aligned}\tilde{X} &= X_i + X_j + \omega X_m \\ \tilde{Y} &= Y_i + Y_j\end{aligned}\tag{1}$$

is added to the set. Thereby the number of vectors in the set is reduced by two. Note that the vectors remain independent after such an operation and that

$$\tilde{X} \geq X_i, X_j, X_m\tag{2}$$

even for  $\omega = -1$ . This step is then iterated until a single vector  $V_N = (X_N, Y_N)$  is left in the set. In this general formulation, the cases  $\omega = 1, -1, 0$  correspond to the three models in the order as they were quoted in the Introduction. Based on the known asymptotical behaviour of  $X_N$  and  $Y_N$  for large  $N$  in the marginal cases  $\omega = -1, 1$ , we expect

$$X_N \sim N^{\alpha_\omega} \quad \text{and} \quad Y_N \sim N^{\beta_\omega}\tag{3}$$

to hold also for intermediate parameter values  $-1 < \omega < 1$  with some exponents  $\alpha_\omega$  and  $\beta_\omega$  that may depend on  $\omega$ .

## 2.2. Continuum formulation

Now, we consider the continuum limit  $N \rightarrow \infty$  and introduce the probability density  $P_\Gamma(X)$  of the primary variable that has the support  $\Gamma \leq X < \infty$  and that depends on the lower boundary  $\Gamma$  as a parameter. The function  $P_\Gamma(X)$  is normalised as  $\int_\Gamma^\infty P_\Gamma(X)dX = 1$  for any  $\Gamma$ . Following Ref. [7], we consider, furthermore, the expected value  $\bar{Y}_\Gamma(X)$  of the secondary variable under the condition that the primary variable is  $X$ . In the continuum limit, the system is described by these two functions of  $X$ , which depend on the lower boundary of the support  $\Gamma$  as a parameter. The inequality (2) implies that, as the fraction of vectors  $c_\Gamma$  that have not yet been eliminated decreases in the course of the coagulation process, the lower edge  $\Gamma$  of the distribution continuously increases. As it is shown in the Appendix, one may write the following differential equation for  $P_\Gamma(X)$ :

$$\frac{\partial P_\Gamma(X)}{\partial \Gamma} = P_\Gamma(\Gamma)\Theta[X-(2+\omega)\Gamma] \int_\Gamma^{X-(1+\omega)\Gamma} P_\Gamma(X')P_\Gamma(X-X'-\omega\Gamma)dX', \quad (4)$$

where  $\Theta(X)$  is the Heaviside step function. The fraction  $c_\Gamma$  is related to  $\Gamma$  as  $dc_\Gamma/c_\Gamma = -2P_\Gamma(\Gamma)d\Gamma$  or, equivalently,

$$\frac{dc_\Gamma}{d\Gamma} = -2P_\Gamma(\Gamma)c_\Gamma. \quad (5)$$

The function  $Q_\Gamma(X)$  defined as

$$Q_\Gamma(X) \equiv P_\Gamma(X)\bar{Y}_\Gamma(X), \quad (6)$$

can be shown to obey the differential equation

$$\frac{\partial Q_\Gamma(X)}{\partial \Gamma} = 2P_\Gamma(\Gamma)\Theta[X-(2+\omega)\Gamma] \int_\Gamma^{X-(1+\omega)\Gamma} Q_\Gamma(X')P_\Gamma(X-X'-\omega\Gamma)dX'. \quad (7)$$

The derivation of this equation is given again in the Appendix.

## 2.3. Fixed point solution

In the marginal cases  $\omega = -1, 1$ , it is known that, for any well-behaving initial distributions  $\rho(X, Y)$  with finite moments, the solutions of Eqs. (4) and (7) tend to a universal fixed point solution  $P_\Gamma^*(X)$ ,  $Q_\Gamma^*(Y)$  in the limit  $\Gamma \rightarrow \infty$  that has the scaling property

$$\begin{aligned} P_\Gamma^*(X) &= \Gamma^{-1}f(X/\Gamma) \\ Q_\Gamma^*(X) &= \Gamma^{\delta_\omega-1}g(X/\Gamma), \end{aligned} \quad (8)$$

with some number  $\delta_\omega$  that is related to the growth exponents as $\ddagger$

$$\delta_\omega = \beta_\omega/\alpha_\omega. \quad (9)$$

Therefore we expect this to hold also for intermediate parameter values  $-1 < \omega < 1$  with some (a priori unknown) exponent  $\delta_\omega$  that may depend on  $\omega$ . Indeed, the functions

$\ddagger$  This can be seen from the equation  $\bar{Y}_\Gamma^*(\Gamma) \equiv Q_\Gamma^*(\Gamma)/P_\Gamma^*(\Gamma) = \Gamma^{\delta_\omega}g(1)/f(1)$  that indicates the asymptotical relation  $Y \sim X^{\delta_\omega}$  between the typical values of primary and secondary variables.

in Eq. (8) solve Eqs. (4) and (7) provided that the universal scaling functions  $f(x)$  and  $g(x)$  satisfy the following differential equations:

$$\frac{d[xf(x)]}{dx} = -f_1\Theta(x-2-\omega) \int_1^{x-1-\omega} f(x')f(x-x'-\omega)dx' \quad (10)$$

$$\frac{d[x^{1-\delta_\omega}g(x)]}{dx}x^{\delta_\omega} = -2f_1\Theta(x-2-\omega) \int_1^{x-1-\omega} g(x')f(x-x'-\omega)dx', \quad (11)$$

where the notation  $f_1 \equiv f(1)$  has been used. For an alternative derivation of these equations in the case  $\omega = 1$ , see Ref. [7]. Using the fixed point solution, Eq. (5) can be integrated yielding the asymptotic relation in the large  $\Gamma$  limit:

$$\Gamma \sim c_\Gamma^{-\frac{1}{2f_1}}. \quad (12)$$

Comparing this with Eq. (3), we obtain the relation:

$$\alpha_\omega = \frac{1}{2f_1}. \quad (13)$$

### 3. Approximative determination of $\alpha_\omega$

As can be seen, Eq. (10) does not contain  $g(x)$  and together with Eq. (13) it constitutes an autonomous problem for the calculation of the exponent  $\alpha_\omega$ . For the special case  $\omega = -1$ , the solution of Eq. (10) is of simple form:  $f(x) = e^{-x+1}$ ; this yields  $\alpha_{-1} = \frac{1}{2}$ . In the other marginal case,  $\omega = 1$ , the Laplace transform of the solution is known [5, 8] and  $\alpha_1 = 1$ . In the case  $-1 < \omega < 1$ , where Eq. (10) is not soluble, we shall construct an approximative solution that enables us to give an accurate estimate of  $\alpha_\omega$ . An alternative way related to the numerical analysis of the Laplace transforms is presented in the next section.

Some properties of the scaling function  $f(x)$  can be easily established by investigating Eq. (10) without knowing the exact solution. Apparently, the r.h.s. of Eq. (10) and, as a consequence,  $f(x)$  is non-analytical at  $x = x_1 \equiv 2 + \omega$ . But, as  $f(x)$  itself appears on the r.h.s. as a convolution with a shifted argument  $x - 1 - \omega$ , the r.h.s. as well as  $f(x)$  must be non-analytical also at  $x = x_2 \equiv x_1 + 1 + \omega$ . Iterating this argument, it turns out that there are infinitely many points where  $f(x)$  is non-analytical. To be precise, one can show by recursion that the  $2n$ th derivative of  $f(x)$  is discontinuous at§

$$x_n = 1 + (1 + \omega)n, \quad n = 0, 1, 2, \dots \quad (14)$$

Furthermore, the function value of  $f(x)$  at some  $x'$  is determined by  $f(x)$  in the restricted domain  $(1, x' - 1 - \omega)$ . Due to this property,  $f(x)$  can be constructed in the intervals  $[x_n, x_{n+1}]$  step by step starting with  $n = 0$ . However, the solution is more and more complicated for increasing  $n$  as it contains multiple integrals that cannot be evaluated

§ For a more direct way to this result in the case  $\omega = 1$ , where the explicit form of the scaling function  $f(x)$  is available, see Ref. [8].

analytically. In the domains  $[x_n, x_{n+1}]$ ,  $n = 1, 2, \dots$ , the function  $f(x)$  can be written in the following form:

$$f(x) = \frac{1}{x} \sum_{i=0}^n f_1^{2i+1} C_\omega^{(2i+1)}(x), \quad x_n \leq x \leq x_{n+1}, \quad (15)$$

whereas  $f(x) = 0$  if  $x < x_0$ . The functions  $C_\omega^{(2i+1)}(x)$  are independent of  $f_1$  and the first three of them read as

$$\begin{aligned} C_\omega^{(1)}(x) &= 1, \\ C_\omega^{(3)}(x) &= -2 \int_{x_1}^x \frac{\ln(x' - \omega - 1)}{x' - \omega} dx', \\ C_\omega^{(5)}(x) &= -2 \int_{x_2}^x \int_{x_0}^{x'-x_2+1} \frac{C_\omega^{(3)}(x' - x'' - \omega)}{x''(x' - x'' - \omega)} dx'' dx'. \end{aligned} \quad (16)$$

Substituting an exponential trial function in Eq. (10), we obtain that the asymptotical solution  $f_\infty(x)$  in the limit  $x \rightarrow \infty$  is of the form

$$f_\infty(x) = \frac{a}{f_1} e^{-a(x+\omega)}, \quad (17)$$

with the some number  $a$  that is not fixed by this substitution. The graph of  $f(x)$  for  $\omega = 0$  is shown in Fig.1. As can be seen,  $f(x)$  tends rapidly to  $f_\infty(x)$  for increasing

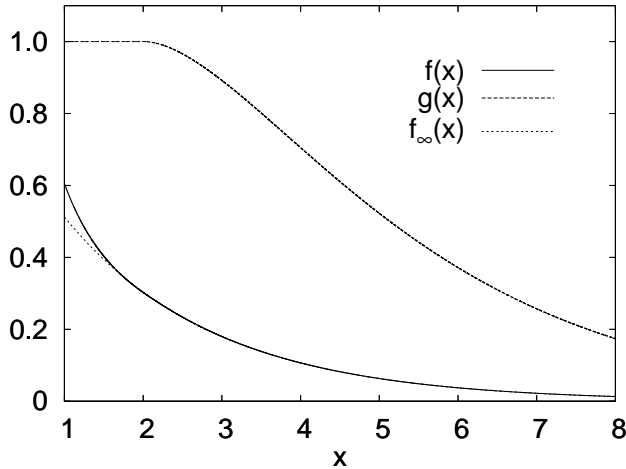


**Figure 1.** Graphs of the functions  $f(x)$ ,  $g(x)$  and  $f_\infty(x)$  for  $\omega = 0$ . The former two are obtained by numerical integration of Eqs. (10) and (11), whereas the latter is given in Eq. (17).

$x$ . This suggests an approximation for  $f(x)$  in which  $f(x)$  is replaced by the simple asymptotical function  $f_\infty(x)$  for large  $x$ . To be precise, the  $n$ th ( $n = 0, 1, 2, \dots$ ) approximant  $f^{(n)}(x)$  is defined as

$$\begin{aligned} f^{(n)}(x) &= f(x), & \text{if } x \leq x_n \\ f^{(n)}(x) &= f_\infty(x), & \text{otherwise.} \end{aligned} \quad (18)$$

The two unknown parameters  $f_1$  and  $a$  are determined by the requirements that  $f^{(n)}(x)$  is continuous at  $x = x_n$ , i.e.

$$f(x_n) = f_\infty(x_n), \quad (19)$$

and that it is normalised as

$$\int_{x_0}^{x_n} f(x)dx + \int_{x_n}^{\infty} f_\infty(x)dx = 1. \quad (20)$$

Using the expression in Eq. (15), straightforward calculations result in that the  $n$ th approximant  $f_1^{(n)}$  ( $n > 0$ ) is the root of the following transcendental equation:

$$\begin{aligned} & \sum_{i=0}^{n-1} [f_1^{(n)}]^{2i+1} C_\omega^{(2i+1)}(x_n) + \\ & + \frac{x_n}{x_n + \omega} \left[ 1 - \sum_{i=0}^{n-1} [f_1^{(n)}]^{2i+1} N_\omega^{(2i+1)}(x_n) \right] \ln \left[ f_1^{(n)} - \sum_{i=0}^{n-1} [f_1^{(n)}]^{2i+2} N_\omega^{(2i+1)}(x_n) \right] = 0, \end{aligned} \quad (21)$$

where the function  $N_\omega^{(2i+1)}(x)$  has been introduced as

$$N_\omega^{(2i+1)}(x) \equiv \int_{x_i}^x \frac{C_\omega^{(2i+1)}(x')}{x'} dx'. \quad (22)$$

We have numerically calculated the root of Eq. (21) and the  $n$ th approximant  $\alpha_\omega^{(n)}$  of  $\alpha_\omega$  by using Eq. (13) for  $n = 1, 2, 3$  and for several values of  $\omega$ . This has necessitated the numerical evaluation of the integrals in Eq. (22) for  $n > 1$ . Results are shown in Fig. 2 and some numerical values are given in Table I. As can be seen, the approximants  $\alpha_\omega^{(n)}$  converge rapidly with increasing  $n$  and they increase monotonically with  $\omega$ . The best estimate for the diameter exponent of the graph cited in the Introduction is  $\alpha_0^{(3)} = 0.82617561$ .

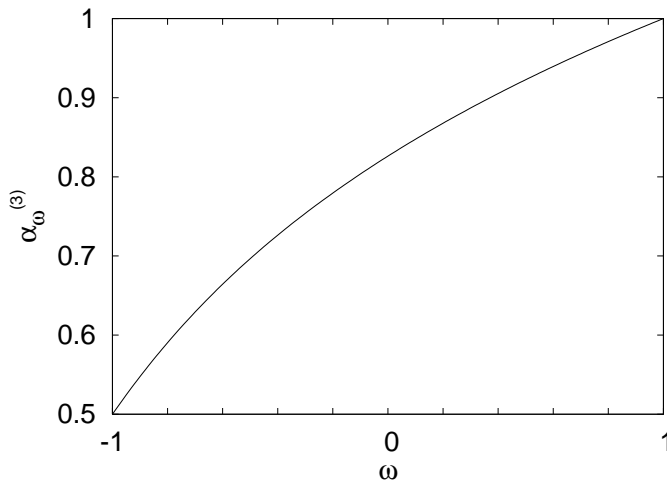


**Figure 2.** The third approximant  $\alpha_\omega^{(3)}$  of the exponent  $\alpha_\omega$  plotted against  $\omega$ .

$\omega$	$\alpha_\omega^{(1)}$	$\alpha_\omega^{(2)}$	$\alpha_\omega^{(3)}$	$\delta_\omega$	$\beta_\omega = \delta_\omega \alpha_\omega^{(3)}$
-0.9	0.54752760	0.54752815	0.54752815	1.48973578	0.81567227
-0.8	0.59036797	0.59037862	0.59037860	1.38841226	0.81968889
-0.7	0.62906729	0.62911723	0.62911708	1.30687751	0.82217896
-0.6	0.66421085	0.66434418	0.66434376	1.23995279	0.82375490
-0.5	0.69632781	0.69659263	0.69659189	1.18399594	0.82476197
-0.4	0.72586754	0.72630756	0.72630667	1.13643762	0.82540221
-0.3	0.75320237	0.75385266	0.75385199	1.09543864	0.82579860
-0.2	0.77863838	0.77952410	0.77952421	1.05965756	0.82602872
-0.1	0.80242716	0.80356405	0.80356560	1.02809664	0.82614309
0.0	0.82477635	0.82617193	0.82617561	0.99999999	0.82617561
0.1	0.84585830	0.84751339	0.84751989	0.97478484	0.82614953
0.2	0.86581708	0.86772721	0.86773715	0.95199472	0.82608118
0.3	0.88477397	0.88693068	0.88694457	0.93126697	0.82598219
0.4	0.90283179	0.90522369	0.90524198	0.91230963	0.82586098
0.5	0.92007834	0.92269199	0.92271501	0.89488491	0.82572374
0.6	0.93658910	0.93940970	0.93943769	0.87879701	0.82557503
0.7	0.95242937	0.95544130	0.95547441	0.86388324	0.82541834
0.8	0.96765597	0.97084323	0.97088154	0.85000684	0.82525595
0.9	0.98231868	0.98566518	0.98570869	0.83705175	0.82508918
1.0	0.99646128	0.99995110	0.99999976	0.82492447	0.82492427

**Table 1.** Approximants of the exponents  $\alpha_\omega$ ,  $\delta_\omega$  and  $\beta_\omega$  for different values of  $\omega$ .

#### 4. Numerical determination of $\beta_\omega$

Next, we turn to the determination of the exponent  $\delta_\omega$  (and, at the same time,  $\beta_\omega$  through Eq. (9)), which requires the analysis of the full problem, i.e. the system of differential equations (10) and (11). Prior to this, a few remarks concerning the scaling function  $g(x)$  are in order. First, as a consequence of the definition in Eq. (6),  $g(x)$  apparently inherits the singularity properties of  $f(x)$  discussed in the previous section. Furthermore, it can be written in a form analogous to Eq. (15). In the domain  $[x_0, x_1]$ , it has a simple form:

$$g(x) = g(1)x^{\delta_\omega - 1}, \quad x_0 \leq x \leq x_1. \quad (23)$$

Second, the differential equation (11) gives the scaling function  $g(x)$  only up to a multiplicative constant. This non-universal constant depends on the initial distribution  $\rho(X, Y)$  and it is fixed in a non-trivial way by the original equations (4) and (7) that are valid for any  $\Gamma$ . Third, the equation (11) contains the a priori unknown parameter  $\delta_\omega$  that must be fixed by physical considerations about the solution that depends on  $\delta_\omega$ . Namely, the physically acceptable solution must be nonnegative and must have the only

reasonable asymptotics allowed by Eq. (11):

$$g_\infty(x) \simeq \text{const} \cdot x e^{-ax}, \quad (24)$$

where the number  $a$  is the same as that appears in Eq. (17). Numerical analysis of Eq. (11) shows that these requirements are fulfilled only for a single value of the parameter  $\delta_\omega$ .

Following Ref. [7], it is, however, simpler to analyse the Laplace transform of the equations (10) and (11). Introducing the functions

$$\phi(p) = \int_1^\infty e^{-px} f(x) dx, \quad \psi(p) = \int_1^\infty e^{-px} g(x) dx, \quad (25)$$

the equations (10) and (11) transform to

$$p\phi'(p) = f_1[e^{-\omega p}\phi^2(p) - e^{-p}], \quad (26)$$

$$p\psi'(p) = -\delta_\omega\psi(p) - g_1e^{-p} + 2f_1e^{-\omega p}\psi(p)\phi(p), \quad (27)$$

where the prime denotes derivation by  $p$  and  $g_1 \equiv g(1)$ . These equations are not soluble in the parameter range  $-1 < \omega < 1$  but asymptotical expressions of the solution can be established. The functions  $\phi(p)$  and  $\psi(p)$  have the small- $p$  expansions:

$$\phi(p) = \sum_{n=0}^{\infty} a_n p^n, \quad \psi(p) = g_1 \sum_{n=0}^{\infty} b_n p^n. \quad (28)$$

Substituting these into Eqs. (26) and (27), we obtain that the expansion coefficients for  $-1 < \omega < 1$  are given by  $a_0 = 1$ ,  $b_0 = \frac{1}{2f_1 - \delta_\omega}$  and by the following recursion relations for  $n > 0$ ||:

$$a_n = \frac{\frac{(-1)^n}{n!}(\omega^n - 1) + \sum_{0 \leq i, j, k < n; i+j+k=n} \frac{(-\omega)^i}{i!} a_j a_k}{\frac{n}{f_1} - 2} \quad (29)$$

$$b_n = \frac{\frac{(-1)^n}{n!} \left( \frac{\omega^n}{2f_1 - \delta_\omega} - \frac{1}{2f_1} \right) + \frac{1}{2f_1 - \delta_\omega} a_n + \sum_{0 \leq i, j, k < n; i+j+k=n} \frac{(-\omega)^i}{i!} a_j b_k}{\frac{n + \delta_\omega}{2f_1} - 1}. \quad (30)$$

Next, we discuss the large- $p$  behaviour of  $\psi(p)$ . The differential equation (27) can have two kinds of asymptotical solutions depending on the parameter  $\delta_\omega$ . If the second term on the r.h.s. dominates, we obtain

$$\psi'(p) \simeq -g_1 \frac{e^{-p}}{p}, \quad (31)$$

while, if the first term dominates, we obtain

$$\psi(p) \simeq \text{const} \cdot p^{-\delta_\omega}. \quad (32)$$

On the other hand, it follows from Eq. (25) that  $\psi(p)$  must have the large- $p$  asymptotics:  $\psi(p) \simeq g_1 e^{-p}/p[1 + O(1/p)]$ . Using that the function  $g(x)$  is explicitly known in the domain  $1 \leq x \leq 2 + \omega$  (see Eq. (23)), we can obtain a more accurate asymptotical form

|| These series expansions are also valid for  $\omega = -1$  with  $a_2 = 5/2$ , and for  $\omega = 1$  with  $a_1 = -2e^\gamma$  [7], where  $\gamma$  is Euler's constant, given by  $\gamma = -\int_0^\infty \ln t e^{-t} dt = 0.577215 \dots$

for  $1/p \ll 1 + \omega$ . Replacing  $g(x)$  by the function in Eq. (23) in the entire domain  $x \geq 1$ , the integral in Eq. (25) can be evaluated, yielding

$$\psi_\infty(p) = g_1 e^{-p} \sum_{k=0}^{\infty} \binom{\delta_\omega - 1}{k} \frac{k!}{p^{k+1}}, \quad p \gg \frac{1}{1 + \omega}. \quad (33)$$

This shows that the physically acceptable asymptotics is that given in Eq. (31) whereas that in Eq. (32) is non-physical. Numerical analysis of the differential equations (26) and (27) with the correct value of  $f_1$  shows the following behaviour of the solution when the parameter  $\delta_\omega$  is varied: For small enough  $\delta_\omega$ , the function  $\psi(p)$  is non-monotonous and tends to zero from below for increasing  $p$  as given in Eq. (32); for large enough  $\delta_\omega$ , the function  $\psi(p)$  decays monotonically to zero again with the asymptotics given in Eq. (32). These parameter regimes are separated by a ‘‘critical’’ value of  $\delta_\omega$ . At this value, the solution decays monotonically to zero with the physically acceptable asymptotics given in Eq. (31).

The numerical estimation of  $\delta_\omega$  is based on this scenario: The differential equations (26) and (27) are integrated from  $p = 0$  to some large  $p$  and the true value of  $\delta_\omega$  is selected by the condition that  $\psi(p)$  has the correct asymptotics. We have assumed here that  $f_1$  is already at our disposal. This can be obtained either by the approximative procedure described in the previous section or, analogous to the above method, from the condition that  $\phi(p)$  has the correct asymptotics given by Eq. (33) with  $\delta_\omega = 0$ .

Before presenting numerical results on  $\delta_\omega$ , we show that, in the case  $\omega = 0$ , the assumption on the uniqueness of the value  $\delta_\omega$  that corresponds to the correct asymptotics implies that  $\delta_0 = 1$ . For  $\omega = 0$ , the primary and the secondary variables coagulate according to the same rules, see Eq. (1). If these variables are initially perfectly correlated, i.e.  $X_i = bY_i$  with some common constant  $b$  for all  $i$ , it is obvious that  $\alpha_0 = \beta_0$ . Nevertheless, this equality holds for general initial distributions, as well. Indeed, it is easy to check that for  $\omega = 0$ , the function

$$\psi(p) = -\frac{g_1}{f_1} \phi'(p) \quad (34)$$

solves Eq. (27) provided that  $\delta_0 = 1$  and  $\phi(p)$  is the solution of Eq. (26). In terms of the scaling functions, equation (34) reads as  $g(x) = x f(x) \frac{g_1}{f_1}$ . As the asymptotics of the solution in Eq. (34) is physically acceptable, we conclude that

$$\delta_0 = 1. \quad (35)$$

The details of the numerical determination of  $\delta_\omega$  are the followings. The best approximant that we have,  $f_1^{(3)}$ , has been substituted in Eqs. (26) and (27) and a trial value for  $\delta_\omega$  has been chosen. As the derivatives  $\phi'(p)$  and  $\psi'(p)$  calculated from these equations are of the form  $0/0$  at  $p = 0$ , the functions  $\phi(p)$  and  $\psi(p)$  were first calculated at  $p = 0.05$  by using the small- $p$  expansion in Eq. (28) in order to avoid numerical uncertainties of the integration in the vicinity of  $p = 0$ . Then, starting from  $p = 0.05$ , the differential equations were integrated by the Bulirsch-Stoer method [14] to some  $p_f$ , where  $\psi(p_f)$  is compared to the asymptotical form in Eq. (33). In practice, we have monitored the derivative  $\psi'(p_f)$  rather than  $\psi(p_f)$  and  $p_f = 12$  was sufficiently large so

that the asymptotical value (at the critical  $\delta_\omega$ ) is reached within the numerical accuracy of the integration. The true  $\delta_\omega$  was then selected by the condition  $\psi'(p_f) = \psi'_\infty(p_f)$ . The exponent  $\delta_\omega$  determined in this way is plotted against  $\omega$  in Fig. 3 whereas  $\beta_\omega = \delta_\omega \alpha_\omega^{(3)}$  is plotted against  $\omega$  in Fig. 4. Some numerical values can be found in Table 1. As can be seen,  $\delta_\omega$  decreases monotonically with  $\omega$  but  $\beta_\omega$  has a maximum at  $\omega = 0$ . The latter observation will be explained in the next section.

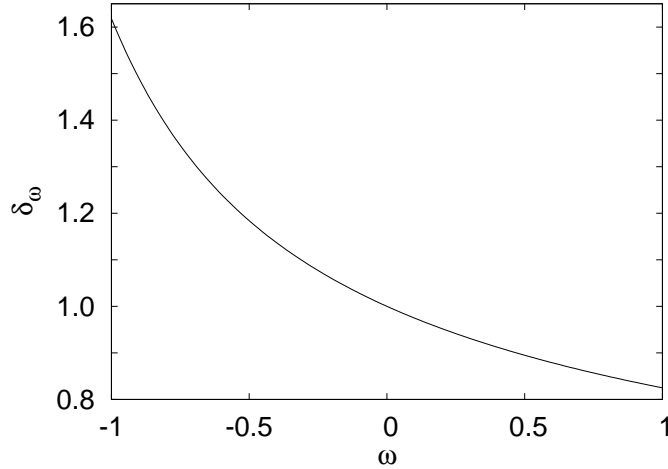


**Figure 3.** Numerically calculated exponent  $\delta_\omega$  plotted against  $\omega$ .

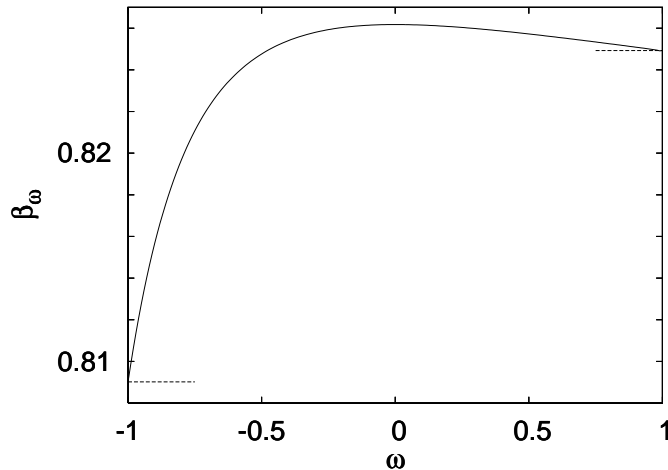


**Figure 4.** Numerically calculated exponent  $\beta_\omega = \delta_\omega \alpha_\omega^{(3)}$  plotted against  $\omega$ . The horizontal lines indicate known values in the marginal cases  $\omega = -1, 1$ .

## 5. Discussion

We have shown that two problems, the renormalisation group procedure of certain disordered quantum spin chains and a simple model describing coarsening in the

Glauber-Ising model can be deformed into each other by varying a single parameter. The interpolating model is a special type of non-conserving coagulation process where only the actually smallest mass is active. In the range  $-1 \leq \omega \leq 1$ , the exponents  $\alpha_\omega$  and  $\beta_\omega$  that characterise the growth of the primary and the secondary variables, respectively, vary continuously with  $\omega$ . The latter exponent exhibits a maximum, which contrasts with the monotonous dependence of the generalised persistence exponent on the partial survival factor that appears directly in the transformation rule of the secondary variable [10]. Although, we have focused on the range  $-1 \leq \omega \leq 1$ , the equations written down in this work are valid also for  $\omega > 1$ . In that case, the growth of the primary variable becomes super-linear, meaning that  $\alpha_\omega > 1$ .

An intriguing feature of the process studied in this work is the universality with respect to the initial distribution of the variables: For a fixed  $\omega$ , any sufficiently rapidly decaying initial distribution tends at late times to a universal distribution that displays scaling. Although, the process is universal in this sense, we have pointed out that it is sensitive to the variations of the reaction rules parameterised by  $\omega$ . The dependence of  $\alpha_\omega$  on  $\omega$  is obvious since the transformation rule of the primary variable contains  $\omega$  explicitly. The growth of the secondary variable is, however, affected by  $\omega$  in a more subtle way. Focusing on the secondary variables, the difference to the process of primary variables with  $\omega = 0$  is that, here, not exactly the smallest variable is removed from the set. This is the reason for that  $\beta_\omega$  is unequal to  $\alpha_0$  for  $\omega \neq 0$ . Nevertheless, for any  $\omega$ , the removed secondary variable is typically relatively small since  $X_i$  and  $Y_i$  become positively correlated in the course of the process. Due to these correlations, the strength of which is controlled by  $\omega$ , the variation of  $\beta_\omega$  is relatively slight. Indeed, it is by an order of magnitude smaller than that of  $\alpha_\omega$ .

For  $\omega = 0$ , we have shown that  $\alpha_0 = \beta_0$  even if the primary and the secondary variables are initially not perfectly correlated. This can be understood also on a microscopic level since, in this case, the vectors in the set are sums of an increasing number of initial vectors. Thus, the ratios  $\tilde{X}_i/\tilde{Y}_i$  tend stochastically to a common constant in the limit  $\Gamma \rightarrow \infty$  for all  $i$ . In words, the two types of variables become asymptotically perfectly correlated for  $\omega = 0$ . Now, we are in a position to understand why the exponent  $\beta_\omega$  is maximal at  $\omega = 0$ . At that point, the correlations are (at least asymptotically) perfect and almost always the smallest one among the secondary variables is removed. For  $\omega \neq 0$ , however, the correlations are no longer perfect and, as a consequence, not strictly the smallest secondary variables are eliminated. Therefore the fastest growth of  $Y$  is realized at  $\omega = 0$ .

In a general aspect, the benefit of the analysis carried out in this work is that the numerical technique developed here for obtaining accurate estimates of the growth exponents may also apply to other non-soluble coagulation processes with extremal dynamics.

## Appendix A.

When the primary variables in the infinitesimal interval  $(\Gamma, \Gamma + d\Gamma)$  are eliminated in the course of the process, we may write for the change of the probability density  $P_\Gamma(X)$ :

$$P_{\Gamma+d\Gamma}(X) = \left\{ P_\Gamma(X) + P_\Gamma(\Gamma)d\Gamma \int dX_1 \int dX_2 P_\Gamma(X_1)P_\Gamma(X_2) \right. \\ \left. [\delta(X - X_1 - X_2 - \omega\Gamma) - \delta(X - X_1) - \delta(X - X_2)] \right\} \frac{1}{1 - 2P_\Gamma(\Gamma)d\Gamma}. \quad (\text{A.1})$$

Here, the first term of the integrand is related to the newly generated primary variable while the other two terms are related to the removed ones. The factor  $1/[1 - 2P_\Gamma(\Gamma)d\Gamma]$  ensures that the distribution remains normalised. Expanding the l.h.s. of Eq. (A.1) and retaining only terms of order  $d\Gamma$ , we arrive at the differential equation (4).

The expected value  $\overline{Y}_\Gamma(X)$  of the newly generated secondary variable under the condition that the generated primary variable is  $X$  is given as

$$\overline{Y}_\Gamma(X) = \left\{ \int dX_1 \int dX_2 [\overline{Y}_\Gamma(X_1) + \overline{Y}_\Gamma(X_2)] P_\Gamma(X_1)P_\Gamma(X_2) \delta(X - X_1 - X_2 - \omega\Gamma) \right\} / I_\omega(X) = \\ 2 \int_\Gamma^{X-(1+\omega)\Gamma} dX' P_\Gamma(X') \overline{Y}_\Gamma(X') P_\Gamma(X - X' - \omega\Gamma) / I_\omega(X), \quad (\text{A.2})$$

for  $X > (2 + \omega)\Gamma$ , where the function  $I_\omega(X) \equiv \int_\Gamma^{X-(1+\omega)\Gamma} dX' P_\Gamma(X') P_\Gamma(X - X' - \omega\Gamma)$  has been introduced. The expected value  $\overline{Y}_{\Gamma+d\Gamma}(X)$  can then be written as the weighted average of  $\overline{Y}_\Gamma(X)$  and  $\overline{Y}_{\Gamma+d\Gamma}(X)$  as follows:

$$\overline{Y}_{\Gamma+d\Gamma}(X) = \frac{[P_\Gamma(X) - 2d\Gamma P_\Gamma(\Gamma)P_\Gamma(X)] \overline{Y}_\Gamma(X) + d\Gamma P_\Gamma(\Gamma) I_\omega(X) \overline{Y}_{\Gamma+d\Gamma}(X)}{P_\Gamma(X) + d\Gamma P_\Gamma(\Gamma) [I_\omega(X) - 2P_\Gamma(X)]}. \quad (\text{A.3})$$

This leads to the differential equation

$$\frac{\partial P_\Gamma(X) \overline{Y}_\Gamma(X)}{\partial \Gamma} = P_\Gamma(\Gamma) \Theta [X - (2 + \omega)\Gamma] I_\omega(X) \overline{Y}_{\Gamma+d\Gamma}(X), \quad (\text{A.4})$$

where we have made use of Eq. (4). Rewriting this equation in terms of  $Q_\Gamma(X)$  given in Eq. (6), one arrives at Eq. (7).

## Acknowledgments

The author thanks F. Iglói for useful discussions. This work has been supported by the Hungarian National Research Fund under grant no. OTKA K75324.

## References

- [1] Bray A J, 1994 *Adv. Phys.* **43** 357
- [2] Derrida B, Godrèche C and Yekutieli I 1990 *Europhys. Lett.* **12** 385  
Derrida B, Godrèche C and Yekutieli I 1991 *Phys. Rev. A* **44** 6241
- [3] Wattis J A D, McCartney D G and Gudmundsson T 2004 *J. Eng. Math.* **49** 113

- [4] Deloubrière O, Hilhorst H J and Täuber U C 2002 *Phys. Rev. Lett.* **89** 250601
- [5] Nagai T and Kawasaki K 1986 *Physica A* **134** 483
- [6] Kawasaki K, Ogawa A and Nagai T 1988 *Physica B* **149** 97
- [7] Bray A J, Derrida B and Godrèche C 1994 *Europhys. Lett.* **27** 175
- [8] Rutenberg A D and Bray A J 1994 *Phys. Rev. E* **50** 1900
- [9] Bray A J and Derrida B 1995 *Phys. Rev. E* **51** R1633
- [10] Majumdar S N and Bray A J 1998 *Phys. Rev. Lett.* **81** 2626
- [11] Ma S-K, Dasgupta C and Hu C-K 1979 *Phys. Rev. Lett.* **43** 1434  
For a review, see: Iglói F and Monthus C 2005 *Phys. Rep.* **412** 277
- [12] Fisher D S 1992 *Phys. Rev. Lett.* **69** 534  
Fisher D S 1994 *Phys. Rev. B* **50** 3799  
Fisher D S 1995 *Phys. Rev. B* **51** 6411
- [13] Juhász R 2008 *Phys. Rev. E* **78** 066106
- [14] Press W H, Teukolsky S A, Wetterling W T and Flannery B P 1992 *Numerical Recipes in C*  
Cambridge University Press, Cambridge